Mechanochromic Response of 3D Composite Photonic Crystals by Numerical Simulation

Valentina Piccolo[1], Alessandro Vaccari[2], Andrea Chiappini[3], Cristina Armellini[3], Luca Deseri[1,4,5], Maurizio Ferrari[3] and Daniele Zonta[6,3]

[1]DICAM-University of Trento, Via Mesiano 77, Trento, 38123, Italy
[2]Fondazione Bruno Kessler, Via Sommarive, 14, 38123, Trento, Italy
[3]IFN-CNR CSMFO Lab &FBK CMM, Via alla Cascata 56/C, 38123 Trento, Italy.
[4]MEMS-Swanson School of Engineering, Univ. of Pittsburgh Benedum Hall, 3700 O'Hara Street, Pittsburgh, USA
[5]Dept. of Mech.Eng Dept. Carnegie Mellon University, Pittsburgh PA 15213-3890 USA
[6]University of Strathclyde, Montrose Street, 75, Glasgow, G1 1XJ, Scotland, UK

Abstract

In this work, we present the possible use of 3D Photonic Crystals in Structural Health Monitoring. We show how the optical response of a colloidal photonic crystal built from sub-micrometric polystyrene spheres in a PDMS matrix on a rubber substrate varies with elongation. The optical features are analyzed by means of Finite Difference Time Domain (FDTD) three-dimensional (3D) simulations, using an in-house code that numerically solves Maxwell's equations for a light beam impinging on the crystal. It contains different wavelengths in the visible spectrum and the wave amplitudes of the reflected and transmitted secondary beams are then observed. A change in the characteristic prominently reflected or transmitted wavelengths is produced, ascribable to changes in the spacing between the spheres due to deformation. This behavior is ultimately amenable to diffractive effects from the crystal, which are fully captured by our full wave 3D FDTD model. It uses the basic equations governing the light-matter interaction at a macroscopic level, without any simplifying approximations. Further numerical studies are in progress to compare the proposed computational model with the experimental results. Nowadays numerical investigations are a powerful and important tool in predicting and studying the behavior of a real sensor device, for which the experimental data of interest are not always clearly recognizable because of complexity.

1. Introduction

Measuring the strain field of a structural component is one of the key task in Structural Health Monitoring (SHM). Currently, the most commonly used techniques for obtaining strain data are optical fiber Bragg grating and electronic strain gauges [(1-6)], but a major limitation to the widespread application of SHM are additional costs of the sensor network and the particular specialization for the data analysis. In order to monitoring large areas an innovative and low cost technology is required. Strain imaging could be one of the possible way, in fact photo-mechanics offers new possibilities in terms of full-field measurement techniques that could have a great impact on the mechanical

characterization of materials and structures. In this research field, there are many techniques to visualize strain distribution of deforming structure, i.e. moiré interferometry, holography, image analysis, speckles and etc. [7]. Engineering a new class of nanostructured optical materials, as sensing elements in smart systems, could lead to the development of new devices for stress and strain sensing.
Between these new mechano-chromatic materials, in this paper the use of colloidal mechano-chromic photonic crystals [8-12] is proposed. A photonic crystal (PhC) is a periodic structure with nanometric periodicity. In this particular case the periodicity is comparable with the wavelength of light, that means having a photonic band gap in the visible range: in practice, it reflects selectively only a band of the incident light, thus appearing to the observer of a determinate color. The idea of using PhC as strain sensor is based on the observation that any distortion in the crystal structure produces a change in the reflected bandwidth, resulting in turn in a change in its apparent color, visible to naked eyes. The envisaged goal, in a near future, is to be able to spread a photonic sensitive material on the surface of a structure in the form of a thin paint layer, providing in this way efficient, effective inspection and monitoring capabilities to assess infrastructure damage that can be safely used by untrained end users. In the next section the basic formulation that controls the photomechanical behaviour of 3D photonic structures is briefly recalled. After that, a Finite Difference Time Domain (FDTD) analysis method to simulate the opto-mechanical response of a generic photonic crystal design, through direct integration Maxwell's equations, is presented. Lastly, the feasibility of the fabrication of a PhC made of sub-micrometric polystyrene colloidal spheres in a poly-dimethylsiloxane (PDMS) matrix on a rubber substrate is reported and the good agreement between the experimental results and the numerical model is shown. Some concluding remarks are reported at the end of the paper

2. Approximation of the optical behaviour with linear elasticity

To explain the general theory behind the optical behaviour of the envisaged device, a 3D photonic crystal, made of colloidal spheres in an elastomeric matrix having refractive indices n_1 and n_2 respectively, and filling factor f, is considered. Sending a white light with zero incidence angle to the crystal, it gets reflected at a wavelength λ. As a first approximation this wavelength can be evaluated by employing the Bragg's law [13]:

$$\lambda = 2 \cdot n_{eff} \cdot d \,, \tag{1}$$

where d is the interplanar distance of the spheres and n_{eff} is the effective refractive index of the crystal, which is evaluated through a mixture theory approximation as follows:

$$n_{eff}^2 = f \cdot n_1^2 + (1-f) n_2^2 . \tag{2}$$

Hence, a "small" change of the quantity d will result in a change in the reflected wavelength according to the following formulation:

$$\Delta\lambda = 2 \cdot n_{eff} \cdot \Delta d = 2 \cdot n_{eff} \cdot d_0 \cdot \varepsilon_3 , \tag{3}$$

where ε_3 is the crystal (small) strain in the orthogonal direction to its plane and d_0 is the interplanar spacing in the referential configuration, meaning the unstrained condition.

This method applies in the context of infinitesimal strain. In a real working condition, the crystal is adherent to a substrate and, for the sake of convenience to better explain the working principle, it is considered to be subjected to a plain stress condition. Obviously the vertical contraction is related to the two in-plane strain components of the substrate through the following relationship:

$$\varepsilon_3 = -\frac{\nu}{1-\nu}\{\varepsilon_1 + \varepsilon_2\}. \tag{4}$$

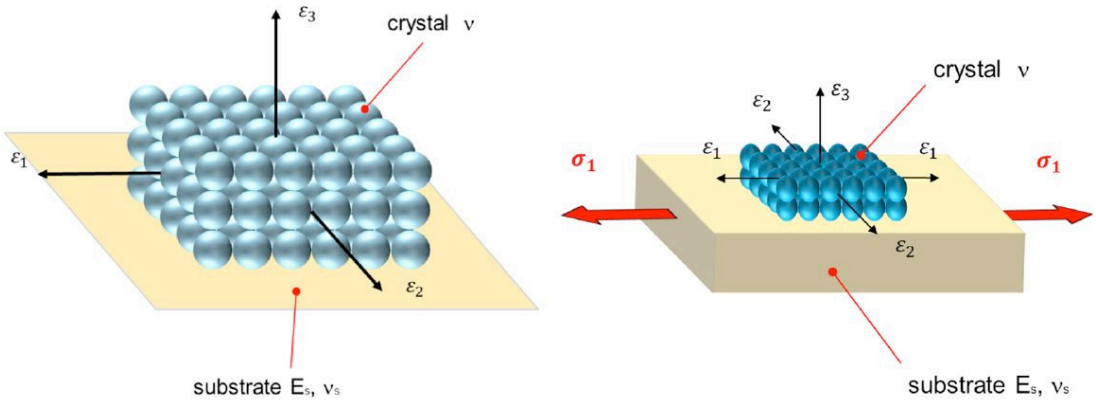

(a) (b)

Figure 1. (a) A three dimensional photonic crystal on the substrate in the reference configuration; (b) the direction of the applied stress (σ_1) and the related strain distribution (ε_1, ε_2, ε_3) are shown; E_s, ν_s are Young modulus and Poisson's ratio for substrate, ν Poisson's ratio for photonic crystal.

If a stress σ_1 is applied to the substrate in direction 1 as shown in fig. 1, this will result in an elongation in the same direction and in two contractions in the two orthogonal directions. With the assumption of effective isotropy of the composite, the strain in the same plane of the substrate, ε_2, can be evaluated with the following formula:

$$\varepsilon_2 = -\nu_s \varepsilon_1, \tag{5}$$

where ν_s is the Poisson's coefficient of the substrate. Replacing (5) in (4), it results:

$$\varepsilon_3 = -\nu \frac{1-\nu_s}{1-\nu}\varepsilon_1 \approx -\nu\varepsilon_1, \tag{6}$$

where the approximation is valid as long as the two Poisson's ratios are close enough. Equation (6) states that when the substrate is stretched under a uniaxial stress in one in-plane direction, the crystal contracts approximately ν times the elongation along the stress direction. Combining (6) with (3), the following expression for change in the reflected wavelength $\Delta\lambda$, is determined:

$$\Delta\lambda \approx -2 \cdot n_{eff} \cdot \nu \cdot d_0 \cdot \varepsilon_1. \tag{7}$$

Probably, the assumption of having an isotropic response is a too crude approximation, although this point will be discussed in sect. 4. But, both the refractive index n_{eff} and Poisson's ratio ν change with strain. Henceforth, the relationship between the bandgap

wavelength and the transverse strain becomes nonlinear. In this case the sensitivity of $\Delta\lambda$ with the change in longitudinal strain takes approximately the following form:

$$\frac{\mathrm{d}\lambda}{\mathrm{d}\varepsilon_1} \approx -2 \cdot d_0 \cdot \left\{ \frac{\mathrm{d}n_{eff}}{\mathrm{d}\varepsilon_1} \cdot \nu \cdot \varepsilon_1 + n_{eff} \cdot \frac{\mathrm{d}\varepsilon_3}{\mathrm{d}\varepsilon_1} \right\}. \tag{8}$$

By making the assumption of a linearly elastic behavior of the material and the effective refraction index n_{eff} constant with strain, equation (8) reduces to the following expression:

$$\frac{\mathrm{d}\lambda}{\mathrm{d}\varepsilon_1} \approx -2 \cdot n_{eff} \cdot \nu \cdot d_0, \tag{9}$$

which basically shows that the crystal sensitivity to strain is proportional to its refractive index, lattice spacing and Poisson's ratio.

3. The optical response of the crystal by numerical simulations

The simplified mathematical model described in sect. 2 has been implemented in a numerical code based on the Finite Difference Time Domain (FDTD) method. The purpose here is twofold. On the one end, it shows the goodness of the approximated theory described above. On the other end, this sets the stage for a preliminary understanding of the weakly-coupled optomechanical behavior of this highly complex physical system. This methodology indicates the direction to the design of innovative photonic sensors. This group has already validated this numerical method in several other papers [14-16], writing a specific code in order to better represent the physics of the problem involved.

Here, the progressive displacement of the PS spheres inside the PDMS matrix has been modeled. At each step, that stands for the position reached by the spheres during the deformation of the device, the exciting signal is a linearly polarized plane wave pulse, injected on the FDTD grid by means of the so called total-field/scattered-field (TF/SF) method that represents the monochromatic light.

The parameters that have been used in the simulation are taken from the realized sample described in the next section, meaning spheres with a diameter of 230 nm with an interplanar spacing of 280 nm inside a PDMS matrix. Here, the simplifying assumption of nonabsorbitive materials and no substrate under the crystal have been made. The latter has been modeled with 12 planes in z direction, and it is infinite in the x and y directions.

As shown in fig. 4, a change in the reflectance is observed at every programmed step in which there is a variation in the distance between the spheres, that means varying the lattice constant of the crystal structure (the values of the distance between the spheres is listed at the side of the graph). A change in this latter parameter means a change in the geometry, which directly impact on the filling factor that in turn, as shown in formula (2), implies a change in the effective refractive index. The calculated sensitivity is around 3.85 με /pm.

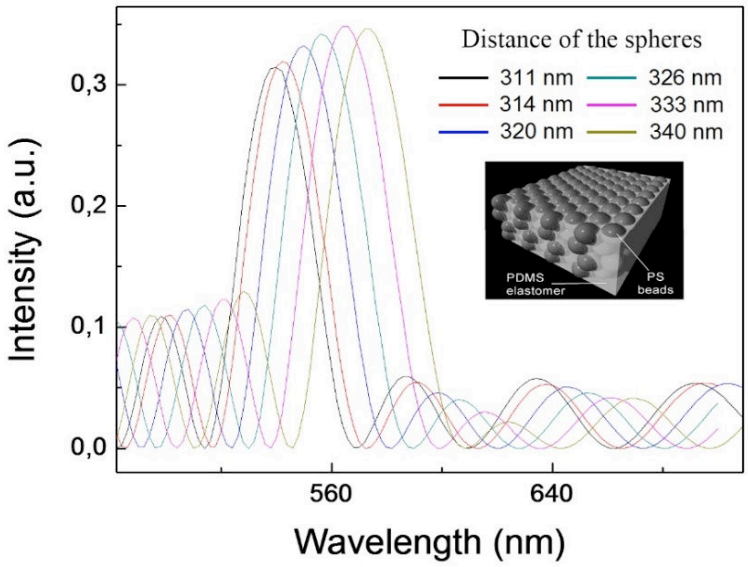

Figure 2. Reflectance spectra of the numerical simulations.

4. Fabrication of the sample and validation of the simulations

The sample was produced by using the classic vertical deposition technique (one can find the details in [17]), among the other available techniques. The crystal is composed by polystyrene spheres (PSs) infiltrated with poly-dimethylsiloxane (PDMS). The fabrication process is basically characterized by three steps: the formation of the PSs, the vertical deposition of the latter in the support (Viton substrate of size 50x15x1mm) arranged in a lattice structure (fcc) and the infiltration with the elastomer.
In order to work in the visible range, the spheres have been made with a diameter of 230 nm and an interplanar spacing, after the last cycle of infiltration, of 280 nm, fig. 3a) shows a SEM image of the structure. With these parameters a bandgap wavelength of 582nm is obtained.
During the test, the substrate strip was fastened to two micrometric linear stages, as shown in [10], and stretched in uniaxial condition to different strain levels, the experimental setup is shown in fig. 3b). At each step, the reflectance of the PhC was recorded using a spectrometer with a wavelength resolution of 0.1 nm. Fig. 4a) shows the reflectance obtained for different values of the longitudinal strain, while fig. 4b) plots the experimental relationship between reflectance peak wavelength and strain.
As predicted by Equation (9), the wavelength decreases with the applied strain and, below 120 mε, the relationship is approximately linear. In particular, the experimental sensitivity to strain and its inverse are:

$$\frac{d\lambda}{d\varepsilon} = -0.288 \text{ pm}/\mu\varepsilon\,, \qquad \frac{d\varepsilon}{d\lambda} = -3.47 \ \mu\varepsilon/\text{pm}. \tag{10}$$

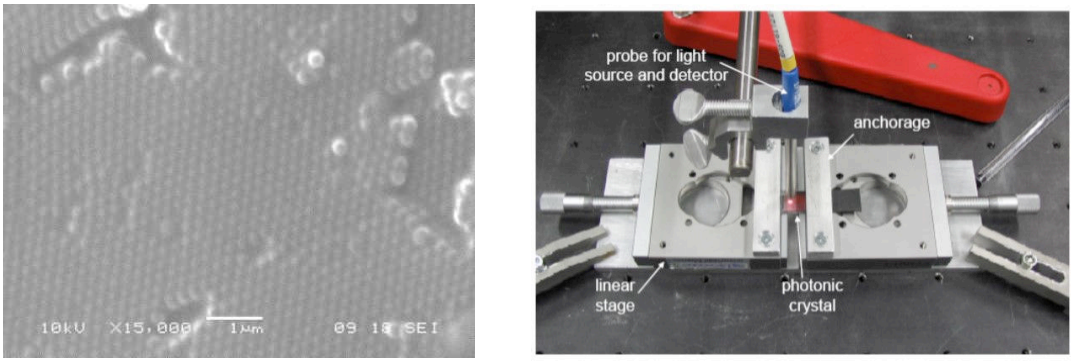

Figure 3. (a) Scanning Electron Microscopy (SEM) picture of the crystal and (b) test setup [10].

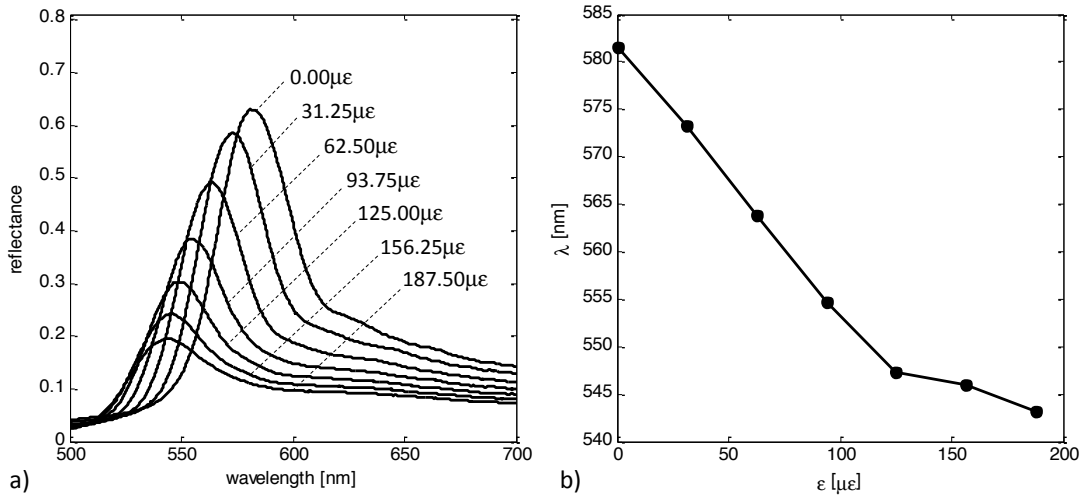

Figure 4. Reflectance spectra (a) of the colloidal PhC recorded during the elongation test and (b) experimental relationship between bandgap wavelength and strain.

If the maximum reflectance peak can be resolved with an accuracy of 0.1 nm, this corresponds to instrumental resolution of about 350 με. Such a resolution is acceptable for applications where the strain to be measured is a few percent. The latter circumstance though would invalidate the assumption of geometric linearity, namely infinitesimal strains, and also the material response would, at the very least, be nonlinearly elastic. Nonetheless such accuracy is actually not sufficient for civil and mechanical engineering applications, where a strain resolution the order of 5 με is typically required.

Equation (9) suggests that the resolution could be easily improved by increasing the crystal interplanar spacing, for example by changing the size of the beads and/or by multiplying the swelling/infiltration cycles. However, this will result in a crystal which does not work in the visible range. Such a device has then to be interrogated exclusively with instrumentation, thereby losing the feature that makes it appealing for monitoring applications.

4.1 Comparison between the experimental results and the numerical simulations

Comparing the behaviour of the numerical results with the experimental ones, it is clear that there is a shift in the reflected wavelength from the higher to the lower ones. This effect is in agreement with the statement expressed in formula (7). This shift shows also a decrease in the intensity, nonetheless the position peak is almost identical. From a phenomenological point of view, the decrease in the reflection intensity is proportional to the ratio between the difference of the refractive index of the materials (which is assumed to be constant in the model) and the effective refractive index, as shown in the following formula [18].

$$I \propto \frac{\Delta n}{neff} \tag{11}$$

This demonstrates that the effective refractive index is changing due to the change in the volume fraction of the system. Such a volume fraction for the FCC lattice can be evaluated as follows [19]:

$$f = \frac{2\pi}{3}\frac{d^3}{a^3} \tag{12}$$

where d is the diameter of the spheres and a is the lattice parameter ($a=d_{111}\sqrt{3}$).
A possible explanation for the fact that in the experiments the intensity decreases faster is that in the calculated numerical reflectance the absorbed power has been neglected because there is not the imaginary component of the refractive index.
The asymmetry in the shape of the reflection spectra in the experiments is probably due to the cracks that are present into the sample [20]. The effects of this defects are unavoidable while measuring, since the illuminated area is much larger (the unit are millimeters squared) than the domain without them (of the order of micrometers). Those cracks, which arises during the drying process of the PhC films, are not entirely avoidable and some other groups are working on this fabrication problem [21-23].
The shape of the experimental spectra changes also with the applied strain showing a broadening of it. This behaviour is probably due to the coexistence of two phenomena that happen during the deformation of the sample: the opening of the cracks described above and an inhomogeneous differential displacement of the different planes of the crystal. This latter aspect could lead to an analogy with the reflectance spectra of a heterostructure [24-26], where there is the convolution of the contributions that every different inner structure gives. The numerical results coming from this approximated treatment of the problem do not exhibit the broadening of the spectra. This could be explained with the assumption of a homothetic expansion of the spheres at each step, not taking into account the possible inhomogeinities of the strain field in the matrix across neighboring spheres,as well as boundary effects of the substrate into the crystals that could lead to a non-homogeneous displacements of the spheres in all directions and, obviously, the assumption of a perfect structure without any defects.
From the practical point of view, the key aspect for SHM is the sensitivity of a strain sensor. As we highlighted in section 3, the sensitivity of our device was around 3.5 με /pm and it results in good agreement with the numerical one, which is around 3.85 με /pm. We can state with confidence that, not only from this point of view, the two

systems are almost the same and the numerical model approximates at the best the experiment.

5. Conclusions

The presented results of the numerical simulations obtained by an approximate linear elastic model, with the further approximation of the homothetic expansion of the spheres, with no inhomogeinities on the strain field, is already in agreement with what it was than seen experimentally and with the analytical model presented in sect. 2. Although a more refined model is required in order to set a robust understanding of the performances of the device, the device has a preliminary validation for the envisioned applications. These systems could be integrated into the assessment of the risk level of individual structures: on the one hand, they will be able to support the decision-making process to establish the restoration project and on the other, they will allow a more robust estimation of the effectiveness of the restoration works. Summing up, the realization of this kind of structures is highly innovative and will develop low-cost devices for the on-line monitoring of deformative state of civil structures. Moreover, they will provide an immediate response to the opening of cracks, are almost non-invasive, and are designed to work without the need of an external power supply.

Acknowledgements

The research activity is performed in the framework of Centro Fermi MiFo project.

References

1. R. M. Measures, 'Structural monitoring with fiber optic technology', Academic Press, 2001.
2. B. Glisic, D. Inaudi, 'Fiber optic method for structural health monitoring', Wiley, 2007.
3. M. Pozzi, D. Zonta, H. Wu, D. Inaudi, 'Development and laboratory validation of in-line multiplexed low-coherence interferometric sensors', Optical Fiber Technology, 14: 281–293, 2008.
4. D. Zonta, B. Glisic, S. Adriaenssens, 'Value of information: impact of monitoring on decision-making', Structural Control and Health Monitoring, 21: 1043–1056, 2014.
5. C. Cappello, D. Zonta, M. Pozzi, R. Zandonini, 'Impact of prior perception on bridge health diagnosis', Journal of Civil Structural Health Monitoring, 5: 509–525, 2015.
6. C. Cappello, D. Zonta, B. Glisic, 'Expected utility theory for monitoring-based decision making'. Proceedings of the IEEE, 2016.
7. C. A. Sciarella, 'Overview of optical techniques that measure displacements: Murray lecture', Experimental Mechanics 43(1), 2003.
8. A. Chiappini, C. Armellini, A. Chiasera, M. Ferrari, Y. Jestin, M. Mattarelli, M. Montagna, E. Moser, G. Nunzi Conti, S. Pelli, C. G. Righini, M. C. Gonçalves, R. M. Almeida, 'Design of photonic structures by sol–gel-derived silica nanospheres', Journal of Non-Crystalline Solids, 353: 674-678, 2003.

9. H. Fudouzi, T. Sawada, 'Photonic rubber sheets with tunable color by elastic deformation'. Langmuir, 22: 1365-1368, 2006.
10. H. Fudouzi, 'Soft opal films with tunable structural color and their applications'. Proceedings of SPIE, 6005: 22-30, 2005.
11. D. Zonta, A. Chiappini, A. Chiasera, M. Ferrari, M. Pozzi, L. Battisti, M. Benedetti, 'Photonic crystals for monitoring fatigue phenomena in steel structures'. Proceedings of SPIE, 7292 729215/1-10, 2008.
12. Z. M. Wang, A. Neogi, 'Nanoscale Photonics and Optoelectronics'. Springer, 2010.
13. R. M. Almeida, S. Portal, 'Photonic band gap structure by sol-gel processing'. Current Opinion in Solid State & Material Science, 7: 151-157, 2003.
14. A. Vaccari, A. Calà Lesina, L. Cristoforetti, A. Chiappini, F. Prudenzano, A. Bozzoli, and M. Ferrari, 'A parallel computational FDTD approach to the analysis of the light scattering from an opal photonic crystal', Proceedings of SPIE 8781, 87810P-1/6, 2013.
15. A. Vaccari, L. Cristoforetti, A. Calà Lesina, L. Ramunno, A. Chiappini, F. Prudenzano, A. Bozzoli, L. Calliari, 'Parallel finite-difference time-domain modeling of an opal photonic crystal', Optical Engineering 53, 071809-1/6, 2014.
16. A. Vaccari, A. Calà Lesina, L. Cristoforetti, A. Chiappini, L. Crema, L. Calliari, L. Ramunno, P. Berini, and M. Ferrari, 'Light-opals interaction modeling by direct numerical solution of Maxwell's equations', Optics Express 22, 27739-27749, 2014.
17. A. Chiappini, A. Piotrowska, M. Marciniak, M. Ferrari, D. Zonta, 'Design and fabrication of mechanochromic photonic crystals as strain sensor'. Proceedings of SPIE. 9435, 94350J-1/13, 2015.
18. T. Ding, S. K. Smoukov, J. J. Baumberg, 'Stamping colloidal photonic crystals: a facile way towards complex pixel colour patterns for sensing and displays', Nanoscale, DOI: 10.1039/c4nr05934d, 2014.
19. R. D. Pradhan, I. I. Tarhan, G. H. Watson, 'Impurity modes in the optical stop bands of doped colloidal crystals', Physical Review B, 54(19), 1996.
20. Y. A. Vlasov, V. N. Astratov, A. V. Baryshev, A. A. Kaplyanskii, O. Z. Karimov, M. F. Limonov, 'Manifestation of intrinsic defects in optical properties of self-organized opal photonic crystals', Physical Review E, 61(5), 2000.
21. B. Hatton, L. Mishchenko, S. Davis, K. H. Sandhage, J. Aizenberg, 'Assembly of large-area, highly ordered, crack-free inverse opal films', Proceedings of the National Academy of Sciences U. S. A., 107(23):10354-10359, 2010.
22. J. Zhou, J. Wang, Y. Huang, G. Liu, L. Wang, S. Chen, X. Li, D. Wang, Y. Song, L. Jiang, 'Large-area crack-free single-crystal photonic crystal via combined effects of polymerization-assisted assembly and flexible substrate', NPG Asia Materials, 4(e21), 2012.
23. Y. Huang, J. Zhou, B. Su, L. Shi, J. Wang, S. Chen, L. Wang, J. Zi, Y. Song, L. Jiang, 'Colloidal photonic crystals with narrow stopbands assembled from low-adhesive superhydrophobic substrates', Journal of American Chemical Society, 134(41):17053-17058, 2012.
24. H. S. Lee, R. Kubrin, R. Zierold, A. Y. Petrov, K. Nielsch, G. A. Schneider, M. Eich, 'Photonic properties of titania inverse opal heterostructures', Optical Material Express, 3(8), 2013.
25. A. Chiappini, C. Armellini, N. Bazzanella, G. C. Righini, M. Ferrari, 'Opal-based photonic crystals heterostructures', Optics and Photonic Journal, 2: 206-210, 2012.
26. D. K. Hwang, H. Noh, H. Cao, R. P. H. Chang, 'Photonic bandgap engineering with

inverse opal multi-stacks of different refractive index contrast', Applied Physics Letter, 95, 2009.